Structures, Energies, and NMR Shieldings of Some Small Water Clusters on the Counterpoise Corrected Potential Energy Surface

D. B. Chesnut*

P. M. Gross Chemical Laboratory, Duke University, Durham, North Carolina 27708

Received: March 21, 2002; In Final Form: May 8, 2002

The structures of water clusters varying in size from $n = 2$ to $n = 6$ (cyclic, prism, and cage isomers) have been redetermined on a counterpoise-corrected potential energy surface and result in oxygen−oxygen distances that are some 0.1 Å longer than would otherwise be found. NMR shielding calculations have also been carried out on the reoptimized structures and show that the shieldings of the hydrogen bonded protons tend to reproduce the gas-to-liquid shielding change observed for water, whereas those for oxygen do not. Use of the COSMO self-consistent reaction field to determine additional shielding changes does not significantly improve the situation.

Introduction

Water clusters with a small number of waters (2−20) have been of great interest for some time now. Several reviews discuss their structures and properties,[1−3] and a number of recent key papers[4−6] contain very useful references and data that illustrate the complexities in the larger clusters ($n \geq 6$). Beyond the classic C_s water dimer with a single hydrogen bond, the clusters of size $n = 2-5$ are generally agreed to have a cyclic ring structure as their low energy form where adjacent nonbonding hydrogen atoms tend to orient to opposite sides of the ring. At $n = 6$ a number of low energy isomers appear, and the structures at this size and beyond tend to assume more of a three-dimensional character.

Using rather large basis sets and geometries optimized at a MP2(FC)/TZ2P++ level, Kim and Kwang[4] found the $n = 6$ cage conformer lowest in energy, followed closely by the book (within 0.1 kcal/mol) and prism (within 0.2 kcal/mol) structures. These authors included zero-point energy corrections (ZPE) as well as a single, post-optimization basis set superposition error (BSSE) counterpoise correction.[7]

Similar results were found by Xantheas[5] who studied cooperativity in the hydrogen bonded networks in water clusters using MP2(FULL) with the aug-cc-pVDZ basis.[8,9] Counterpoise-corrected energies showed the $n = 6$ prism to be the lowest in energy followed closely by the cage and book forms; the inclusion of ZPE then placed the cage structure lowest. Xantheas pointed out the cooperative effects in the cyclic clusters as revealed by a systematic contraction of the O−O separation[10] and the red shift of the hydrogen bonded OH stretch with increasing cluster size.[10,11]

Maheshwary et al.[6] used a "computationally manageable" 6-31G(d,p) basis at both RHF and B3LYP[12,13] levels of theory to study larger clusters from $n = 8$ to $n = 20$ and found the most stable geometries to arise from fusion of tetrameric or pentameric rings. They also studied the smaller clusters, and, like others, found the $n = 6$ prism to be the lowest in energy in the absence of the ZPE correction, the cage form being the lowest when ZPE energies are included. They also demonstrate that the O−O separations actually increase at the $n = 6$ cluster size and maintain more or less a uniform behavior at higher n.

It is well-known that the calculation of aggregation energies tend to provide too large a result due to basis set superposition error (BSSE),[14,15] and that a method like the counterpoise method of Boys and Bernardi[7] is needed to correct this artificial effect. Up until recently, the counterpoise correction was applied in a single step *after* the optimization (a posteriori) of the molecular aggregate. This does not represent the proper counterpoise corrected potential energy surface, however, because BSSE is not taken into account in the optimization. Significant changes in optimized geometries can occur using the new and correct formulation of Simon, Duran, and Dannenberg[16,17] in which the optimization is carried out explicitly containing the counterpoise correction. This is particularly so for relatively shallow potential energy minima such as those found in hydrogen bonded systems. Employing the counterpoise corrected potential energy surface results in intermolecular distances that tend to be larger and aggregate energies of formation that are greater (more negative).

In the present study, we have reoptimized the $n = 2-6$ water clusters starting from literature examples and explicitly containing the counterpoise correction.[16] This optimization on the counterpoise-corrected potential energy surface results in oxygen−oxygen distance that are some 0.1 Å longer than would otherwise be found. We also find, in agreement with Maheshwary et al.,[6] that the oxygen−oxygen bond distances increase on the average in the $n = 6$ clusters compared to those of smaller size. Although the water clusters are of intrinsic interest in themselves, they have often been looked upon as giving some insight into the structure and properties of liquid water. In this regard then, we thought it would also be interesting to determine their NMR shieldings for the unique $n = 2-5$ cyclic species and the prism, cage, and cyclic hexameric species and compare them to what is known for gaseous and liquid water. We find that the shieldings for the hydrogen bonded protons tend to reproduce the experimental gas-to-liquid shielding change observed for water while those for oxygen do not.

Theoretical Methods

All the energy and frequency calculations were carried out at the MP2(FC)/6-311+G(d,p) level with the Gaussian 98 suite

* To whom correspondence should be addressed. Phone: 919-660-1537. Fax: 919-660-1605. E-mail: dbc@chem.duke.edu.

10.1021/jp020776h CCC: $22.00
Published on Web 06/21/2002

TABLE 1: Interatomic Distances (*R*, Å) between Oxygen Atoms Involved in Hydrogen Bonds for Cluster Geometries with No Counterpoise Correction (ncp) and with Counterpoise Correction (cp), and Distance Differences (Δ*R*, Å)[a]

n		R_{ncp}	R_{cp}	ΔR
2		2.917	3.025	0.108
3		2.799 ± 0.005	2.885 ± 0.033	0.086 ± 0.003
4		2.751	2.845	0.094
5		2.736 ± 0.008	2.834 ± 0.007	0.099 ± 0.002
6	cyclic	2.725	2.822	0.097
	cage	2.825 ± 0.108	2.915 ± 0.104	0.090 ± 0.011
	prism	2.852 ± 0.095	2.943 ± 0.095	0.091 ± 0.007

[a] Standard deviations of the distributions are shown; *n* represents the cluster size.

of programs.[18] Because the $n = 6$ isomers are so close in energy we found it useful to initially optimize those structures using a Z-matrix with a somewhat constrained symmetry, and then removing the constraints with the final optimization carried out in unconstrained Cartesian coordinates.

The NMR determinations used a particular mixture of RHF-(FULL) and MP2(FULL)/6-311+G(d,p) approaches with Ditchfield's gauge invariant atomic orbital (GIAO) method[19] in what we have called the estimated Møller−Plesset infinite order (EMPI) shielding.[20] We found that in many cases the Møller−Plesset series of corrections appears to converge in a manner that allows the infinite series to be summed (approximately), so that the EMPI shielding is given by

$$\sigma_{EMPI} = \sigma_{RHF} + \frac{2}{3}(\sigma_{MP2} - \sigma_{RHF}) \qquad (1)$$

Function counterpoise optimizations (and frequency determinations) used the approach of Simon, Duran, and Dannenberg.[16] No counterpoise corrections were made to the shielding, although this can be of concern when determining changes in shielding anisotropies.[21] Here, for the counterpoise geometry of the water dimer, NMR counterpoise corrections were found to be less than 2.0 ppm for oxygen and less than 0.25 for hydrogen.

Shieldings are on an absolute scale such that more positivie shielding (and positive shielding changes) are considered diamagnetic, whereas more negative shieldings (and negative shielding changes) are considered paramagnetic.

Results and Discussion

Structures and Energies. Although our purpose here is not to explicitly study in a detailed way the relative energies of the various water clusters, it is still important to report our results, especially because the correct counterpoise corrected potential energy surface has been employed.

Table 1 reports the mean oxygen−oxygen distances, a key geometric parameter and basically the only notable bond distance change. Aside from the unique bond in the water dimer and the equivalent distances in the cyclic S_4 tetramer and the cyclic S_6 hexamer, there are a variety of distances in the other species that basically lack symmetry. The distribution of distances is reported as a standard deviation in Table 1 where data from both the counterpoise corrected potential energy surface (cp) and the uncorrected or noncounterpoise surface (ncp) are given. A key observation here is the general increase of about 0.095 Å in O−O distances when the correct potential energy surface is employed, the magnitude of the increase being essentially what Hobza and Havlas report.[17] This is the type of increase in length expected and is significant in magnitude.

SCHEME 1

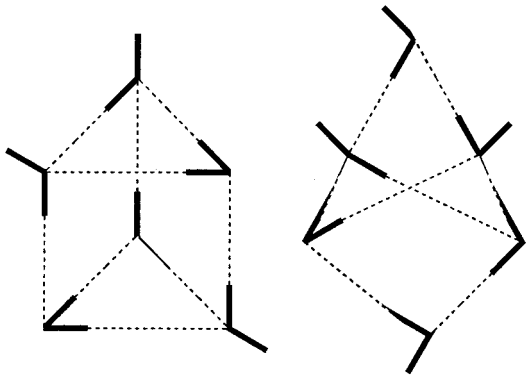

TABLE 2: Energy Changes (Δ*E*, kcal/mol), upon Water *n*-mer Cluster Formation from the Monomeric Species ($E = -76.278\,55$ au) for Clusters Optimized on the Non-Counterpoise Potential Energy Surface ($-\Delta E_{ncp}$), Those Optimized on the Counterpoise Potential Energy Surface ($-\Delta E_{cp}$), and Their Differences ($-\Delta\Delta E$)[a]

n		$-\Delta E_{ncp}$		$-\Delta E_{cp}$		$-\Delta\Delta E$
2		4.44	(1.54)	4.54	(1.30)	0.10
3		13.55	(3.96)	13.83	(3.40)	0.28
4		23.46	(7.36)	24.01	(6.34)	0.55
5		30.88	(10.08)	31.64	(8.50)	0.76
6	cyclic	38.51	(12.30)	39.43	(10.45)	0.92
	cage	38.30	(12.28)	39.29	(10.17)	0.99
	prism	38.52	(12.30)	39.35	(10.64)	0.83

[a] Values in parentheses are the counterpoise correction energies (kcal/mol).

For both types of surfaces the mean O−O distances converge with increasing *n* for the cyclic species but then exhibit an increase in the more three-dimensional cage and prism hexamers. Both these latter structures have increased number of formal hydrogen bonds (8 for the cage, 9 for the prism), but the three-dimensional character of the geometries (shown schematically in Scheme 1) tends to prevent stronger bonds from being formed and longer distances result. These longer distances tend to be the norm as larger and larger clusters are formed.[6] The converging value of the mean oxygen−oxygen distance in the cyclic structures approaches that of liquid water (2.82 Å),[22] but this is misleading because if one averages these distances for the three, larger hexameric species, a significantly higher value (2.893 Å) obtains; the mean of the noncounterpoise-optimized species (2.801 Å) is closer to experiment but this is fortuitous because one is employing an incorrect potential energy surface. The distance reported for ice is 2.74 Å.[23] Our value for the distance in the water dimer of 3.025 Å is larger than that observed from microwave studies of 2.976 Å.[24,25]

Table 2 shows the energy changes upon *n*-mer formation, again for both types of potential energy surfaces. Use of the proper counterpoise corrected potential energy surface results in larger (more negative) stabilization energies, as expected. The counterpoise corrections shown in parentheses are quite large for both types of surfaces. The stabilization energies increase with the number of hydrogen bonds for the cyclic species, but drop off for the cage and prism species, commensurate with the longer mean O−O (and, therefore, hydrogen bond) distances. The change in the stabilization energy moving from the uncorrected to the counterpoise correct potential energy surface tends to behave in a similar manner.

Table 3 shows the absolute and relative energies of the three hexameric species studied here, and is different from the results

TABLE 3: Absolute Electronic (E_{elec}, au) and Zero-Point (E_{ZPE}, au) Energies, Their Individual Relative Values (ΔE^{rel}_{elec}, ΔE^{rel}_{ZPE}, kcal/mol), and Total Relative Energies (E^{rel}_{total}, kcal/mol) for the Cyclic, Cage, and Prism Hexameric Water Clusters. Data are Given for both Geometries Determined on the Counterpoise-Corrected Potential Energy Surface (A) and for Those for Whom the Counterpoise Correction Was Applied a Posteriori (B)

	E_{elec}	ΔE^{rel}_{elec}	E_{ZPE}	ΔE^{rel}_{ZPE}	E^{rel}_{total}
A. counterpoise corrected potential energy surface					
cyclic	−457.73414	0.0	0.14874	0.0	0.0
cage	−457.73392	0.14	0.15064	1.19	1.33
prism	−457.73402	0.08	0.15135	1.64	1.71
B. post-optimization counterpoise corrected geometries					
cyclic	−457.73208	0.39	0.15171	0.0	0.0
cage	−457.73235	0.22	0.15258	0.55	0.38
prism	−457.73270	0.0	0.15311	0.88	0.49

TABLE 4: Isotropic Shieldings for the Counterpoise Corrected Geometries (A, σ_{iso}, ppm) and Differences between Counterpoise-corrected Geometries and Non-Counterpoise-Corrected Geometries (B, $\delta\sigma_{iso}$, ppm) for Hydrogens Not Involved in a Hydrogen Bond (H-nonbonding), Those Involved in a Hydrogen Bond (H-bonding), and Oxygens[a]

A. isotropic shieldings

n		σ_{iso} (H-nonbonding)	σ_{iso} (H-bonding)	σ_{iso} (oxygen)
1		31.36		338.0
2		31.25 (0.43)	28.86	336.2 (1.4)
3		31.16 (0.04)	28.18 (0.07)	331.8 (0.3)
4		31.07	26.69	328.1
5		31.10 (0.06)	26.25 (0.09)	327.4 (0.7)
6	cyclic	31.07	26.04	326.7
	cage	31.02 (0.12)	27.66 (1.28)	325.5 (2.8)
	prism	30.94 (0.07)	28.12 (1.47)	323.4 (3.5)

B. differences in isotropic shieldings between counterpoise-corrected geometries and those geometries uncorrected for bsse.

n		σ_{iso} (H-nonbonding)	σ_{iso} (H-bonding)	σ_{iso} (oxygen)
2		0.05 (0.08)	0.54	1.3 (0.3)
3		0.04 (0.01)	0.69 (0.04)	3.1 (0.1)
4		0.06	1.13	4.6
5		0.05 (0.03)	1.30 (0.02)	6.0 (0.2)
6	cyclic	0.07	1.28	6.0
	cage	0.06 (0.02)	0.89 (0.41)	5.6 (0.9)
	prism	0.05 (0.3)	0.74 (0.38)	5.1 (1.0)

[a] Values in parentheses are standard deviations and give a measure of the range of shieldings and shielding changes for those clusters lacking symmetry.

noted earlier in that the cyclic species is predicted to be the lowest energy isomer of the three. Inclusion of zero-point energies is clearly important, and we note that this correction is smaller when the counterpoise corrected potential energy surface is used. We also observe that the relative ordering of the three species here is independent of the use of the counterpoise corrected potential energy surface. Our results reinforce the fact that the $n \geq 6$ isomers simply lie very close in energy and their relative ordering can well depend on the level of theory and basis set employed.

Isotropic NMR Shieldings. The isotropic shieldings for hydrogen and oxygen are given in Table 4 along with the differences in shielding arising from use of the counterpoise corrected potential energy surface. The changes in shielding in going from the gas to the liquid phase of water are known to be −4.26 ppm for hydrogen[26,27] and −36.1 ppm for oxygen.[28,29] On the basis of our shielding values for gaseous water (the monomer), one then expects a shielding of 27.10 ppm for hydrogen and 301.9 ppm for oxygen in the liquid phase.

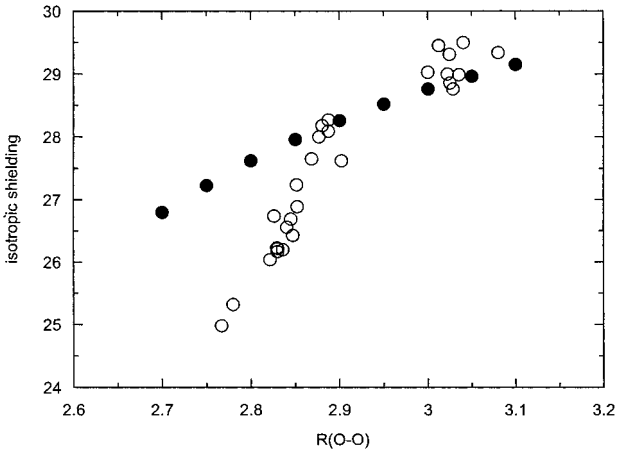

Figure 1. Variation of the isotropic NMR shieldings (ppm) of water cluster hydrogen bonded protons with their associated equilibrium oxygen−oxygen distances (open circles) and of the singular water dimer hydrogen bonded proton as a function of its oxygen−oxygen distance (closed circles).

Several key observations are apparent from part A of Table 4 which presents the absolute shieldings employing the geometries found on the counterpoise corrected potential energy surface. First, the non-hydrogen-bonded hydrogen species show very little shielding change with cluster size, maintaining essentially the gas phase value, as is basically to be expected for protons not involved in hydrogen bonds. On the other hand, the hydrogen bonded species exhibit a monotonic decrease for the cyclic species which then increases for the cage and prism hexamers. The average of the hexameric species is 27.27, which is very close to the experimental change. It seems clear from our results that the formation of the hydrogen bonds is the chief element in shielding change upon formation of the liquid. On the other hand, although the oxygen shieldings show a behavior similar to that of the bonded hydrogens in their dependence on cluster size, the average of the hexameric species is only 325.2, far above the experimentally observed value. One cannot, then, use the water clusters as overall valid models of the liquid state, at least at the size of cluster considered here.

Part B of Table 4 gives the shielding changes between the two potential energy surface geometries. Little effect is seen for the non-hydrogen-bonding hydrogens or, for that matter, for oxygen. Significant changes are seen for those protons involved in hydrogen bonds which, in large part, must arise from the larger O−O distances when the counterpoise corrected potential energy surface is employed. The shieldings, of course, depend on all of the geometrical variables.[30] Figure 1 shows the isotropic shieldings for the hydrogen bonded atoms as a function of their associated O−O distance (open circles) along with the same shieldings for the water dimer (closed circles) where *only* the O−O distance is varied. Clearly, more than just the O−O distance changes are important for those clusters having the shorter hydrogen bonds.

There are other approaches available to mimic the changes seen in the gas-to-liquid phase change. Both self-consistent reaction field (SCRF)[31] and molecular dynamics methods[31,32] have been employed. The early SCRF method used a simple spherical cavity and yielded poor results for a variety of small molecules, not just for species expected to hydrogen bond and for which SCRF methods were really not designed. The molecular dynamics methods showed promise in its initial application[31] and quite good results in extension of that method by Malkin et al.[32] who employed a wider range of potential energy functions. In the molecular dynamics method used by

TABLE 5: Mean Shielding Differences (averaged over all the clusters) from monomeric water for the isolated water clusters ($\Delta\sigma_{isolated}$) and that Obtained with the COSMO Shielding Correction ($\Delta\sigma_{COSMO}$)

	$\Delta\sigma_{isolated}$	$\Delta\sigma_{COSMO}$
oxygen	-9.6 ± 4.0	-5.8 ± 6.0
H (bonding)	-3.96 ± 1.00	-4.04 ± 0.66
H (nonbonding)	-0.27 ± 0.09	-1.46 ± 0.08

Malkin et al., a system of approximately 343 water molecules is equilibrated at $T = 300$ K in a box with periodic boundary conditions. Upon equilibration, the shielding of a central water molecule in clusters of waters ranging in size was then determined quantum mechanically. By also calculating the shielding of the isolated central water molecule one can also separate the liquid-phase shielding into a part due to hydration (hyd) and a part determined by distortion of the molecule from its gas-phase geometry (dis).[31,32] Using a potential due to Li and Clementi[33] for a cluster of size 9 they were able to calculate for hydrogen $\Delta\sigma_{dis} = -0.33 \pm 0.07$, $\Delta\sigma_{hyd} = -2.70 \pm 0.21$, for a total change in shielding of $\Delta\sigma_{tot} = -3.03 \pm 0.20$ ppm, to be compared to the experimental value of -4.26 ppm. Their results for oxygen were $\Delta\sigma_{dis} = -6.0 \pm 1.4$, $\Delta\sigma_{hyd} = -30.4 \pm 2.4$, and $\Delta\sigma_{tot} = 36.4 \pm 2.1$ ppm, compared to the laboratory value of -36.1 ppm. These results are quite good, especially for oxygen, considering the approximations made.

There have been considerable advances in reaction fields so that one might consider retrying this approach. Furthermore, because such methods sometimes involve the solute plus a few molecules of solvation, it would seem appropriate to mimic the hydration of water with water clusters. One of the more successful approaches is the conductor-like solvation model (COSMO) currently implemented in Gaussian 98[18] based on the work of Barone and co-workers.[34,35] It was first proposed by Klamt and Schüürmann[36] for classical calculations and then implemented by Andzelm et al.[37] and Truong and Stefanovich[38] for quantum mechanical calculations. COSMO describes the solvent reaction field by means of apparent polarization charges distributed on a cavity surface of molecular shape formed by interlocking spheres centered on the solute atoms or atomic groups. The polarization charges are determined by requiring the total electrostatic potential on the cavity surface to cancel out.

Because the current Gaussian program does not permit MP2 shielding calculations in the presence of a reaction field, the procedure we followed here was to calculate the isotropic shielding in the B3LYP[12,13] density functional approach with the 6-311+G(d,p) basis both in the presence and absence of the COSMO field and adding that difference to the shieldings obtained at the MP2 level. The results are given in Table 5. The corrections add very little to the hydrogen bonded protons, as might have been expected, but do contribute nearly -1.19 ppm to the nonbonded hydrogens; this latter correction is, however, still too small to account for the experimentally observed shielding change. Furthermore, the oxygen shielding is actually increased (more positive) with the COSMO correction, clearly an undesirable result. We must conclude once again that calculations of NMR shieldings in reaction fields do not account for the experimental results.

Summary

The structures of water clusters varying in size from $n = 2$ to $n = 6$ (cyclic, prism, and cage isomers) have been redetermined on a counterpoise-corrected potential energy surface and result in oxygen−oxygen distances that are some 0.1 Å longer than would otherwise be found. NMR shielding calculations have also been carried out on the reoptimized structures and show that the shieldings of the hydrogen bonded protons tend to reproduce the gas-to-liquid shielding change observed for water but those for oxygen do not. Use of the COSMO self-consistent reaction field to determine additional shielding changes does not significantly improve the situation. In general, we conclude that such water clusters do not represent an overall valid model for NMR shieldings in water's liquid state.

Acknowledgment. I am indebted to the North Carolina Supercomputing Center for providing CPU time on the IBM SP and SGI Origin 2000 platforms that allowed these calculations to be carried out.

References and Notes

(1) Gregory, J. K.; Clary, D. C. *J. Phys. Chem.* **1996**, *100*, 18 014.
(2) Ugalde, J. M.; Alkorta, I.; Elguero J. *Angew. Chem., Int. Ed.* **2000**, *39*, 717.
(3) Müller-Dethlefs, K.; Hobza, P. *Chem. Rev.* **2000**, *100*, 143.
(4) Kim. J.; Kwang, S. K. *J. Chem. Phys.* **1998**, *109*, 5886.
(5) Xantheas, S. S. *Chem. Phys.* **2000**, *258*, 225.
(6) Maheshwary, S.; Patel, N.; Sathyamurthy, N.; Kulkarni, A. D.; Gadre, S. R. *J. Phys. Chem. A* **2001**, *105*, 10 525.
(7) Boys, S. F.; Bernardi, F. *Mol. Phys.* **1970**,*19*, 553.
(8) Dunning, T. H., Jr. *J. Chem. Phys*. **1989**, *90*, 1007.
(9) Kendall, R. A.; Dunning, T. H., Jr.; Harrison, R. J. *J. Chem. Phys*. **1992**, *96*, 6796.
(10) Xantheas, S. S.; Dunning, T. H., Jr. *J. Chem. Phys*. **1993**, *99*, 8774.
(11) Huisken, F.; Kaloudis, M.; Kulcke, A. *J. Chem. Phys*. **1996**,*104*, 17.
(12) Becke, A. D. *J. Chem. Phys.* **1993**, *98*, 5648.
(13) Lee, C.; Yang, W.; Paar, R. G. *Phys. Rev.* **1988**, *B 37*, 785.
(14) Liu, B.; McLean, A. D. *J. Chem. Phys.* **1973**, *59*, 4557.
(15) Liu, B.; McLean, A. D. *J. Chem. Phys.* **1989**, *91*, 2348.
(16) S. Simon, S.; M. Duran, M.; J. J. Dannenberg, J. J. *J. Chem. Phys.* **1996**, *105*, 11 024.
(17) Hobza, P.; Havlas, Z. *Theor. Chem. Acc.* **1998**, *99*, 372.
(18) Frisch, M. J.; Trucks, G. W.; Schlegel, H. B.; Scuseria, G. E.; Robb, M. A.; Cheeseman, J. R.; Zakrzewski, V. G.; Montgomery, Jr., J. A.; Stratmann, R. E.; Burant, J. C.; Dapprich, S.; Millam, J. M.; Daniels, A. D.; Kudin, K. N.; Strain, M. C.; Farkas, O.; Tomasi, J.; Barone, V.; Cossi, M.; Cammi, R.; Mennucci, B.; Pomelli, C.; Adamo, C.; Clifford, S.; Ochterski, J.; Petersson, G. A.; Ayala, P. Y.; Cui, Q.; Morokuma, K.; Malick, D. K.; Rabuck, A. D.; Raghavachari, K.; Foresman, J. B.; Cioslowski, J.; Ortiz, J. V.; Baboul, A. G.; Stefanov, B. B.; Liu, G.; Liashenko, A.; Piskorz, P.; Komaromi, I.; Gomperts, R.; Martin, R. L.; Fox, D. J.; Keith, T.; Al-Laham, M. A.; Peng, C. Y.; Nanayakkara, A.; Gonzalez, C.; Challacombe, M.; Gill, P. M. W.; Johnson, B.; Chen, W.; Wong, M. W.; Andres, J. L.; Gonzalez, C.; Head-Gordon, M.; Replogle, E. S.; Pople, J. A., *Gaussian 98*, revision A.7, Gaussian, Inc., Pittsburgh, PA, 1998.
(19) Ditchfield, R. *Mol. Phys.* **1974**, *27*, 789.
(20) Chesnut, D. B. *Chem. Phys. Lett.* **1995**, *246*, 235.
(21) Chesnut, D. B.; Phung, C. G. *Chem. Phys.* **1990**, *147*, 91.
(22) Narten, A. H.; Levy, H. A. *Science* **1969**, *165*, 449.
(23) Campbell, E. S.; Mezei, M. *Mol. Phys.* **1980**, *41*, 883.
(24) Dyke, T. R.; Mack, K. M.; Muentner, J. S. *J. Chem. Phys.* **1977**, *66*, 498.
(25) Odutola, J. A.; Dyke, T. R. *J. Chem. Phys.* **1980**, *72*, 5062.
(26) Hindman, J. C. *J. Chem. Phys.* **1966**, *44*, 4582.
(27) Raynes, W. T. *Nucl. Magn. Reson*. **1978**, *7*, 1.
(28) Florin, A. E.; Alei, M. *J. Chem. Phys.* **1967**, *47*, 4268.
(29) Raynes, W. T. *Mol. Phys.* **1983**, *49*, 443.
(30) Chesnut, D. B.; Rusiloski, B. E. *J. Phys. Chem*. **1993**, *97*, 2839.
(31) Chesnut, D. B.; Rusiloski, B. E. *J. Mol. Struct. (THEOCHEM)* **1994**, *314*, 19.
(32) Malkin, V. G.; Malkina, O. L.; Steinebrunner, G.; Huber, H. *Chem. Eur. J.* **1996**, *2*, 4452.
(33) Li, G. C.; Clementi, E. *Phys. Rev*. **1986**, *33*, 2679.
(34) Barone, V.; Cossi, M. *J. Phys. Chem. A* **1998**, *102*, 1995.
(35) Rega, N.; Cossi, M.; Barone, V. *J. Comput. Chem.* **1999**, *20*, 1186.
(36) Klamt, A.; Schüürmann, G. *J. Chem. Soc., Perkins Trans*. **1993**, *2*, 799.
(37) Andzelm, J.; Kölmel, C.; Klamt, A. *J. Chem. Phys.* **1995**, *103*, 9312.
(38) Truong, T. N.; Stefanovich, E. V. *Chem. Phys. Lett*. **1995**, *240*, 253.